



## Active control of structures based on an arbitrary damage index distribution

MS. Kazemi<sup>1\*</sup>, F. Behnamfar<sup>2</sup>

<sup>1</sup>Senior Earthquake Engineer, Isfahan, Iran

<sup>2</sup>Department of Civil Engineering, Isfahan University of Technology, Esfahan 8415683111, Iran

**ABSTRACT:** Active control of structures is to keep the dynamic response of stories under a predefined threshold to save the building from excessive damage. Seismic damage has a strong correlation with drift, and control of drift is simply possible in an active control process. Through a regression analysis for many cases, the Park-Ang damage index is approximately re-written based only on story drifts to enhance the common active control procedure to make it able to control the seismic damage. It is shown that the enhanced procedure is successful to keep the damage index values along building height under a predefined distribution. The active control procedure is developed based on the linear quadratic regulator (LQR) algorithm and is used to actively control buildings having up to 10 stories. The target is limiting the story damage index to a prescribed value. Seven consistent earthquake records are used for nonlinear dynamic analysis of concrete structures being 1, 2, 3, 6 and 10 stories in height. The calculated maximum relative difference between the estimated and exact damage indices is shown to be less than 10%. Four earthquake records, different from the suit of ground motions used for developing the damage index equation, are used for testing the developed procedure. It is demonstrated that by using the story drifts estimated by the developed equation, the desired distribution of story damage indices can be established with an excellent accuracy.

### Review History:

Received: 2019-07-03

Revised: 2019-10-19

Accepted: 2019-11-08

Available Online: 2019-12-15

### Keywords:

active control

LQR algorithm

Park-Ang damage index

damage index distribution

drift

## 1. INTRODUCTION

Control of structures against seismic damages is a well established subject. Currently there are four variations of the seismic structural control including passive, hybrid, semi-active, and active control. From the passive control that does not need any external source of energy to be activated, to the active control that may need a large amount of power consumption during a large earthquake, the required level of the supplied energy increases. This shortcoming has made the passive control currently the prime choice when assessing modern techniques for design of a seismic resistant structure. On the other hand, the efficiency of a passive control system depends on the invariant dynamic characteristics of the control system defined for a certain range of systems under ground motions having specific properties. In contrast, the applicability of an active control system is much broader as it is designed to be able to adjust its characteristics during earthquake motions such that it can keep the structural responses under predefined values.

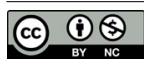
An active control system is generally composed of three parts, including a) sensors to measure structural responses or the external excitations, b) controller computers to process the sensed data and to compute the control forces, and c) actuators to apply the control forces using external power

sources. Various actuators have been used including active bracing, mass damper, or variable stiffness systems. The controlling algorithm of an active control system is another important aspect of its design to be discussed in the next section.

Beginning of modern research on the seismic control of structures dates back to about 40 years ago. Still, it is a highly active area, being the subject of many ongoing tasks. The research works on the active control can be categorized in two broad groups. The first category is related to developing mathematical relations and dynamical equations that govern the active control procedure. It has devoted to the larger part of the related research activities. The main outcome of this part has been developing control algorithms including LQR, LQG, fuzzy logic clipped control, and sliding mode control. In the second category, practical applications of the active control have been the focus of studies. Mainly, it includes tasks in which adjustment of an existing algorithm with some alterations for attaining a specific response reduction has been at stake.

Application of the active control to contain the seismic drift and damage of structures has been the subject of many research works. Yang et al. (1996) achieved practical results in controlling the drift response by using the sliding mode control theory and applying active variable stiffness mechanism. Shooshtari and Saatcioglu (2003) studied an instantaneous

\*Corresponding author's email: farhad@cc.iut.ac.ir



optimal control algorithm to restrain nonlinear response of reinforced concrete structures. The proposed method was promising in control of story drifts and in ductility demand reduction of structural elements. Pang and Wong (2006) used a predictive instantaneous optimal control algorithm to control responses. Their control method was successfully used to restrain floor plastic displacements and member rotations leading to contain the seismic damage. Varasteh et al. (2012) considered the concepts of displacement-based control and modified the LQR algorithm to successfully limit the lateral displacement of the roof of selected structures to a predefined value.

Joghataie and Mohebbi (2012) proposed a nonlinear optimal control algorithm to lower structural responses. Their algorithm was an extension of the nonlinear Newmark integration method combined with a distributed genetic algorithm. Attard and Wharton (2012) applied the controller optimal parameterization algorithm to control displacement and acceleration responses. The algorithm efficiently controlled plastic displacements and plastic strains as factors involved in seismic damage. Baghban et al. (2015) presented an algorithm called NNPC to reduce the nonlinear responses of building structures. They utilized the fragility curves for quantifying the structural damages. KhanSefid and AhmadiZadeh (2016) studied the influence of the extent of the structural nonlinear responses on the performance of the active control system.

Karami and Haghhighipour (2017) used the particles optimization algorithm and the fuzzy logic to achieve a uniform deformation along the structural height. KhanSefid and Bakhshi (2018) developed a two-stage optimization procedure in the LQR algorithm to enhance the structural performances under the main and post earthquake events. In the study by Miamoto et al. (2018), a new performance index has been introduced within the LQR algorithm. The absolute story accelerations, the inter-story drifts and velocities of building floors have been used as the variables in their proposed performance index. They have presented a method for automatic and optimum selection of the weight matrices in the LQR algorithm.

As observed, damage control is currently the result, not the subject, of the active control. This fact is more technological as seismic damage cannot be physically measured and input to an active control system to calculate and apply the associated control forces. On the other hand, the absorbed hysteretic energy in a structure is a more rigorous index to assess its seismic damage. Such a concept is represented by seismic damage indices among them the Park-Ang damage index has attracted a widespread use. Utilizing the mentioned index as the basis of the response control is the main idea in the current study.

In this paper, estimation of the maximum acceptable story drifts is accomplished using an arbitrary drift distribution based on an equation to be derived using the Park-Ang damage index. The LQR control algorithm that is more widely used, is tuned to follow the acceptable drifts and thus the maximum allowable damage indices. Rather than being on

technological or mathematical algorithmic issues, the paper is focused on application of active control to seismic damage control of structures.

## 2. THE DAMAGE INDEX

The level of seismic damage inflicted on a structure is cumulatively identified by a dimensionless factor called the damage index. It is directly dependent on the extent of inelastic deformations along the structural members. Many versions of a damage index have been developed by different researchers. Generally, the maximum deformation or the energy absorbed during the cyclic response at plastic hinges, or a combination of both, are somehow used in damage index equations. One of the most widely used damage indices, especially for reinforced concrete buildings, is that of Park and Ang (Park and Ang, 1985). It is represented by Eq. (1):

$$DI = \frac{\delta_m}{\delta_u} + \frac{\beta}{\delta_u Q_y} \int dE \quad (1)$$

in which  $DI$  is the damage index,  $\delta_m$  is the maximum deformation under earthquake,  $\delta_u$  is the ultimate deformation capacity under monotonic loading,  $Q_y$  is the yield strength,  $\int dE$  is the hysteretic absorbed energy, and  $\beta$  is a non-negative factor indicating effect of the dissipated energy on the extent of damage. Kunnath et al. (Kunnath et al., 1992) used a slightly modified Park-Ang damage index as follows:

$$DI = \frac{\theta_m - \theta_y}{\theta_u - \theta_y} + \frac{\beta}{M_y \theta_u} \int dE \quad (2)$$

in which  $\theta_m$  is the maximum rotation of the section under earthquake,  $\theta_u$  is the ultimate rotation capacity of the section,  $\theta_y$  is the yield rotation of the section, and  $M_y$  is the yield moment.

The damage index, as introduced in Eq. (2), is calculated at the member level. Then it can be determined for a story or a whole structure as follows:

$$DI_{story} = \sum (\lambda_i)_{member} (DI_i)_{member}$$

$$(\lambda_i)_{member} = \left( \frac{E_i}{\sum E_i} \right)_{member} \quad (3)$$

$$DI_{overall} = \sum (\lambda_i)_{story} (DI_i)_{story}$$

$$(\lambda_i)_{story} = \left( \frac{E_i}{\sum E_i} \right)_{story} \quad (4)$$

where  $\lambda_i$  is an energy weight factor and  $E_i$  is the energy absorbed by the  $i$ -th member or story. Equation 2 shows that calculation of the Park-Ang damage index needs knowing the yield and ultimate rotation capacities, and the yield moment, at all of the plastic hinges. It also needs the maximum rotation and the hysteretic absorbed energy under earthquake at each plastic hinge. The latter parameter equals the cumulative area of the hysteretic curves at each plastic hinge. The first three parameters are known before the dynamic analysis because of the known cross section properties. The last two (response) parameters are the output of the structural analysis software.

Based on 82 tests on Caltrans circular bridge columns, the Park-Ang damage index, has been classified as stated in Table 1 (Williams and Sexsmith, 1995).

### 3. THE ACTIVE CONTROL PROCEDURE

#### 3.1. The LQR algorithm

In this research, practical use of an active control system in order to reduce the seismic damage of a structure is considered.

To calculate the control forces, use is made of the well known and wide-spreadly used LQR algorithm. In this algorithm, the control forces vector,  $f(t)$ , is calculated using the following equation:

$$f(t) = -Du(t) \tag{5}$$

where  $u(t)$  is the  $m$ -vector of control forces ( $m =$  number of control forces) and  $D$  is an  $n \times m$  matrix defining the position of the control forces ( $n =$  number of degrees of freedom of structure). Here it is assumed that the control forces are applied at the top of all stories. Their directions are not constant and vary with time, but they act parallel to the earthquake component.

In the active control theory, it is common to develop the equations of motion of the system in the state space. For this purpose, upon defining a  $2n$ -row state vector  $z(t)$  containing  $x(t)$  and  $\dot{x}(t)$  successively as its rows, where  $x(t)$  is an  $n$ -vector representing the structural displacements and  $\dot{x}(t)$  being its derivative, the equation of motion can be written as follows:

$$\dot{z}(t) = Az(t) + Bu(t) + Hf(t) \tag{6}$$

in which:

$$A = \begin{bmatrix} 0 & I \\ -M^{-1}K & -M^{-1}C \end{bmatrix} \tag{7}$$

$$B = \begin{bmatrix} 0 \\ M^{-1}D \end{bmatrix} \tag{8}$$

$$H = \begin{bmatrix} 0 \\ M^{-1}E \end{bmatrix} \tag{9}$$

and  $M$ ,  $C$ , and  $K$  are  $n \times n$  mass, damping, and stiffness matrices of structure, respectively,  $I$  is the unit matrix and  $E$  is an  $n \times r$  matrix defining the external sources of excitation ( $r =$  number of excitations).

To calculate control forces in the LQR algorithm, the performance index,  $J$ , must be minimized as the objective function.  $J$  is defined per Eq. (10):

$$J = \int_0^{t_f} [z^T(t)Qz(t) + u^T(t)Ru(t)] dt \tag{10}$$

in which  $t_f$  is the termination time of application of the control forces,  $Q$  is a positive semi-definite matrix with the dimension  $2n \times 2n$  and  $R$  is a positive definite matrix of  $m \times m$ .  $Q$  and  $R$  are weight matrices determining the relative importance of system and excitation identifiers. They are calculated by trial and error. In this study,  $Q$  and  $R$  are considered to be as follows:

$$Q = I_{2n \times 2n} \tag{11}$$

$$R = m I_{m \times m} \tag{12}$$

where  $m$  represents the weight of control forces with regard to the structural responses. In this study, value of  $m$  has been varied in each case such that the control objective is fulfilled. After selecting the weight matrices and minimizing value of Eq. (10), the vector of control forces is calculated as follows:

$$u(t) = G z(t) \tag{13}$$

where  $G$  is the control gain matrix calculated as follows:

$$G = -\frac{1}{2} R^{-1} B^T P(t) \tag{14}$$

**Table 1. State of damage for each interval of damage index (Williams and Sexsmith, 1995)**

Damage grade	Range of damage index
Collapsed	>0.7
Irreparable	0.4-0.7
Repairable	0.11-0.4
Negligible	0-0.11

in which  $P(t)$  is the Riccati matrix of the system determined from Eq. (15):

$$P = A - \frac{1}{2} PBR^{-1}B^T P + A^T P + 2Q \quad (15)$$

In this study, for calculating the control forces of the system, the initial dynamic properties of the system are utilized. Therefore, the gain matrix will be unchanged during the dynamic excitation. Such a procedure has been conventionally used also by other researchers when working with the LQR algorithm (KhanSefid and Ahmadizadeh, 2016).

### 3.2. The control procedure

Among the possible strategies for adjustment of a control procedure is following an instantaneous approach. As such, in the procedure followed in this paper, the control forces are applied only when a control “switch” is on. The control criterion is whether the story response is crossing a target response or not. In addition to limiting the maximum actions, this approach results in an optimized energy consumption by the control system.

In this research the control criterion is selected to be containing the Park-Ang damage index within a predefined range in each story. The LQR algorithm is adjusted based on this criterion. The problem is that for calculating the plastic energy term in Eq. (1) or (2), availability of rotation values at all of the plastic hinges is necessary. But, measurement of rotations is not a practical task. Instead, first by trial and error and then using a systematic approach, the damage index is limited to the desired value by controlling the story drifts in this research. In the systematic approach, an empirical relation is developed between the story drift and the story damage index.

### 4. THE CASE STUDY BUILDINGS

In this study five regular reinforced concrete structures being 1, 2, 3, 6, and 10 in number of stories are considered.

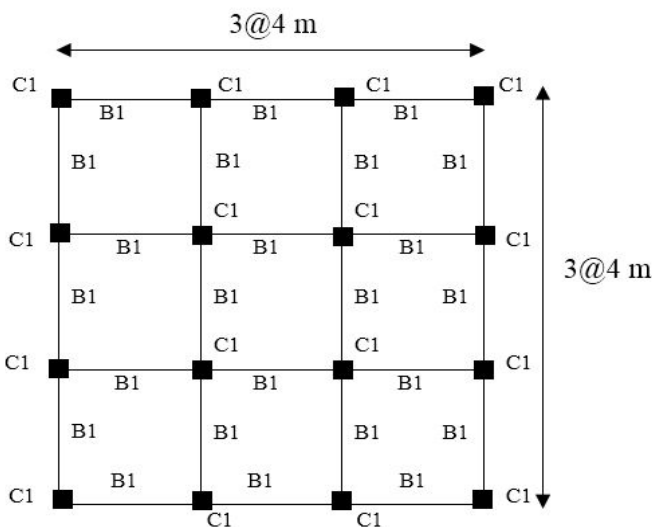


Fig. 1. Plan view of the buildings under study

The residential buildings consist of four intermediate moment frames in each direction with bays spanning 4m both ways, making a 12 m by 12 m plan for all of the stories. Floor to floor heights are 3m identically. For design purposes, a soil type C that is a medium soil according to ASCE 7-10 (ASCE 7-10, 2010) is assumed. The compressive strength of concrete is 30 MPa and the yield strength of rebars is 420 MPa. After structural design, an interior plane frame is picked up for nonlinear analysis and calculation of the damage index. The typical story plan and the dimensions of the structural members are shown in Fig. 1 and Table 2, respectively.

### 5. THE NONLINEAR DYNAMIC ANALYSIS

#### 5.1. Modelling

Each frame is modeled for nonlinear dynamic analysis under a selected suit of ground motions. The Opensees software (OpenSees, 2014) is selected for this purpose. OpenSees possesses a library of constitutive relations for different materials. For concrete, the uniaxial Concrete01 and for steel, the uniaxial Steel01 material models are used. The longitudinal stress-strain relations of the above materials are shown in Fig. 2. As observed, Concrete01 is a Kent-Scott-Park no-tension material behavior with softening and strength degradation in compression. Steel01 exhibits a bi-linear yielding and isotropic strain hardening material behavior common for the mild steel. Beam and column elements are modelled with non-linear beam-column element type that considers the spread of plasticity along the element (Mazzoni et al., 2006). The damping matrix is taken to be of the Rayleigh

Table 2. Cross sections for the members of the buildings (units in centimeters)

(a) 1-story		
Story Number	Column	Beam (bxh)
1	35x35	35x30

(b) 2-story		
Story Number	Column	Beam (bxh)
1-2	35x35	35x30

(c) 3-story		
Story Number	Column	Beam (bxh)
1-3	35x35	35x30

(d) 4-story		
Story Number	Column	Beam (bxh)
1-4	45x45	40x40
5-6	40x40	40x40

(e) 5-story		
Story Number	Column	Beam (bxh)
1-5	50x50	45x50
6-10	45x45	40x50

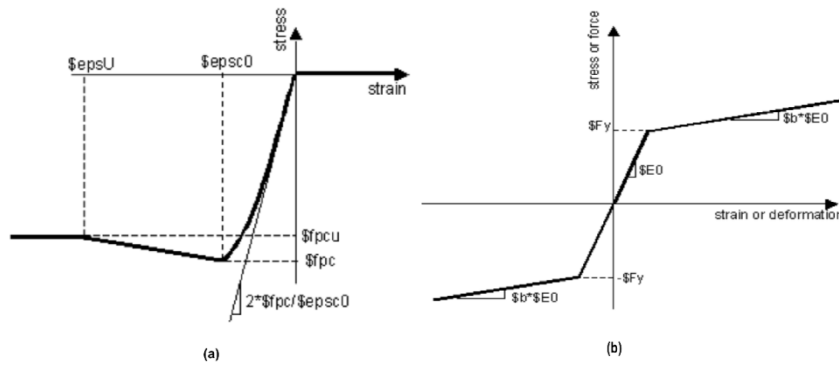


Fig. 2. The stress-strain relations (Mazzoni et al. 2006). (a) Concrete01. (b) Steel01

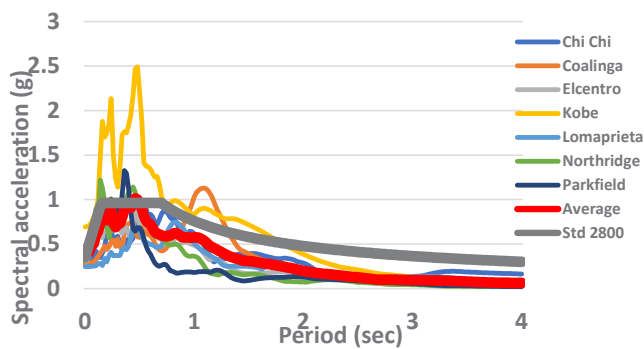


Fig. 3. The un-scaled response spectra along with the average and code-based spectra

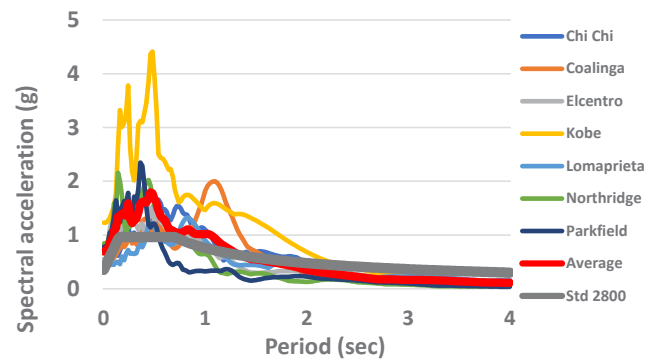


Fig. 4. Scaled response spectra

Table 3. The earthquake records

Earthquake name	Year	Station	PGA (g)
Kobe	1995	CUE 99999 Takarazuka	0.707
Elcentro	1940	USGS 117 Elcentro Array #9	0.258
Coalinga	1983	CDMG 36456 Parkfield	0.271
Chi-Chi	1999	CWB 99999 ChyO36	0.259
Northridge	1994	USG 90091 LA	0.454
Loma prieta	1989	USGS 1028 Hollister City Hall	0.231
Parkfield	1966	CDMG 1014 Cholame- Shandon Array #5	0.377

type and the viscous damping ratio is assumed to be 0.05.

The P-Δ effect is taken into account in the analysis. The step-by-step numerical integration of constant acceleration Newmark scheme is utilized. The appropriate time increment for accuracy appears to be 0.125 times the time step of the earthquake accelerogram by trial and error.

### 5.2. The ground motions selected

For ground motion selection, the PEER NGA strong ground motion database is consulted (PEER, 2014). The selection criteria include: soil type C,  $M > 6$ ,  $PGA > 0.2g$ ,  $10 < R < 50$  km, where  $M$  is the earthquake magnitude,  $PGA$  is the peak ground acceleration,  $g$  is the acceleration of gravity, and  $R$  is distance to the causative fault. For averaging purposes, use of seven records is deemed to be enough (ASCE 2010). Therefore, 7 records have been selected according to

the above criteria as mentioned in Table 3.

The above records are scaled by trial and error in this study such that the whole structure's damage index is larger than 0.7 (corresponding to a severe damage, see Table 1), for each structure. This is meant for the structures to have a considerable nonlinear response under each earthquake and for the control process to exhibit its workability more clearly. The scale factors appear to be 1.4-1.8 in different cases.

The original response spectra of the selected records are shown in Fig. 3. Moreover, the scaled response spectra, for instance for the 10-story building, are shown in Fig. 4.

### 6. THE ACTIVE CONTROL OF DRIFTS

The control procedure, as described in Sec. 3, is implemented to control the structures such that their damage indices are reduced to less than 0.4. According to Table 1, this

maximum acceptable damage index value corresponds to the repairable state of damage. Keeping in mind the practical abilities of the active control sensors, and the emphasis of seismic design codes on reducing the story drifts to contain the seismic damage, the story drift response is selected as the control variable. Accordingly, given the maximum allowable damage index value of 0.4 in the controlled state, the maximum drift value to meet the control objective is obtained in this section by trial and error. It emerges to be between 1.5-3 cm in different cases of buildings. In the next section, a systematic approach is developed for calculating the target drift based on the desired damage index. The control forces are determined using the LQR algorithm and the complete feedback of structural response.

To overcome the problem raised by the time lag between sensing of responses and application of control forces, it is customary to multiply the target drift by a factor smaller

than unity (Chu et al., 2005). For instance, for the 10-story building, the reduction factor proves to be 0.4 for the first and second, 0.5 for the third and fourth, 0.6 for the fifth and sixth, 0.7 for the seventh to ninth, and 0.9 for the tenth story. An alternative approach would be adjusting the entries of the weight matrices of the LQR algorithm and thus the control forces for the same purpose.

The results of damage index control for the five studied buildings under the seven selected earthquake records are listed in Tables 4-8.

The above results show that the utilized control procedure and the drift limitation empirically imposed on stories, have been quite successful in limiting the story damages to the predefined value of 0.4. The problem is how to determine the limiting drift for attaining a desired distribution of damage index along the height of a given building. This issue is addressed in the next section.

**Table 4. Damage indices for uncontrolled (UC) and controlled (C) states of the 1-story building**

Story number	Parkfield		Northridge		Loma Prieta		Kobe		Elcentro		Coalinga		Chi Chi	
	DI		DI		DI		DI		DI		DI		DI	
	UC	C	UC	C	UC	C	UC	C	UC	C	UC	C	UC	C
1	0.95	0.36	0.95	0.33	0.72	0.30	0.95	0.35	0.96	0.34	0.92	0.34	0.92	0.35

**Table 5. Damage indices for uncontrolled (UC) and controlled (C) states of the 2-story building**

Story number	Parkfield		Northridge		Loma Prieta		Kobe		Elcentro		Coalinga		Chi Chi	
	DI		DI		DI		DI		DI		DI		DI	
	UC	C	UC	C	UC	C	UC	C	UC	C	UC	C	UC	C
1	0.87	0.39	0.96	0.24	0.95	0.37	0.95	0.33	0.95	0.31	0.96	0.37	0.95	0.38
2	0.45	0.25	0.45	0.31	0.41	0.21	0.45	0.20	0.42	0.24	0.39	0.25	0.43	0.31
Total	0.78	0.35	0.81	0.27	0.83	0.29	0.85	0.31	0.81	0.27	0.82	0.34	0.81	0.35

**Table 6. Damage indices for uncontrolled (UC) and controlled (C) states of the 3-story building**

Story number	Parkfield		Northridge		Loma Prieta		Kobe		Elcentro		Coalinga		Chi Chi	
	DI		DI		DI		DI		DI		DI		DI	
	UC	C	UC	C	UC	C	UC	C	UC	C	UC	C	UC	C
1	0.81	0.28	0.65	0.38	0.94	0.39	0.94	0.25	0.59	0.32	0.93	0.35	0.57	0.33
2	0.85	0.31	0.96	0.36	0.97	0.36	0.92	0.36	0.96	0.33	0.91	0.37	0.91	0.29
3	0.61	0.20	0.52	0.24	0.53	0.33	0.47	0.18	0.44	0.15	0.40	0.16	0.39	0.12
Total	0.78	0.29	0.78	0.35	0.83	0.37	0.81	0.28	0.76	0.31	0.88	0.35	0.75	0.25

**Table 7. Damage indices for uncontrolled (UC) and controlled (C) states of the 6-story building**

Story number	Parkfield		Northridge		Loma Prieta		Kobe		Elcentro		Coalinga		Chi Chi	
	DI		DI		DI		DI		DI		DI		DI	
	UC	C	UC	C	UC	C	UC	C	UC	C	UC	C	UC	C
1	0.89	0.29	0.85	0.35	0.88	0.31	0.98	0.29	0.97	0.36	0.87	0.33	0.91	0.20
2	0.71	0.23	0.64	0.33	0.78	0.33	0.94	0.32	0.72	0.28	0.94	0.29	0.84	0.20
3	0.67	0.20	0.72	0.32	0.62	0.34	0.91	0.32	0.58	0.26	0.94	0.29	0.68	0.22
4	0.62	0.20	0.59	0.30	0.58	0.33	0.68	0.33	0.54	0.26	0.81	0.27	0.68	0.22
5	0.66	0.24	0.74	0.32	0.59	0.32	0.84	0.35	0.64	0.30	0.71	0.23	0.71	0.21
6	0.45	0.17	0.46	0.24	0.32	0.24	0.57	0.34	0.46	0.26	0.43	0.19	0.54	0.19
Total	0.71	0.22	0.70	0.30	0.71	0.31	0.83	0.33	0.73	0.31	0.85	0.26	0.78	0.20

**7. THE DEVELOPED EQUATION FOR THE DAMAGE INDEX**

The active control based on a prescribed level of acceptable seismic damage is made practical if the maximum story drifts can be estimated using the assumed damage index. Results of Sec. 6 can be used for the same purpose, as follows. As stated in Sec. 6, to arrive at a desired damage index in each story, the studied buildings have been analyzed using nonlinear dynamic analysis under each earthquake repeatedly. The maximum story drift is selected to be the control variable. In each iteration, the maximum drift of the story is varied incrementally (without changing the member sections) and the corresponding maximum damage index is determined. When the desired value of the damage index is fulfilled, the iteration is terminated and the associated story drift is recorded. At the end of calculations, there is a recorded (story drift, damage index) couple at each story. This procedure leads to a linear regression for each story as follows:

$$DI = Au + B \tag{16}$$

where *DI* is the damage index and *u* is the maximum interstory drift. *A* and *B* are factors that vary from story to story. They are determined for each story by regression using the numerical results of Sec. 6 for the controlled state, as follows:

$$\begin{aligned} A &= -0.988n + 21.888 \\ B &= -0.0026n + 0.0281, \quad 1 \leq n \leq 10 \end{aligned} \tag{17}$$

in which *n* is the story number. The upper bound of *n* is taken to be 10, the maximum number of stories investigated in this study.

It is important to note that Eqs. (16) and (17) have been developed for the controlled case. In other words, the numerical values of structural response, when it is actively controlled, have been used for regression. It should be obvious because the purpose in this section is determining the maximum acceptable drifts based on the known damage indices to be input as controlling criteria to the active control process.

**Table 8. Damage indices for uncontrolled (UC) and controlled (C) states of the 10-story building**

Story number	Parkfield		Northridge		Loma Prieta		Kobe		Elcentro		Coalinga		Chi Chi	
	DI		DI		DI		DI		DI		DI		DI	
	UC	C	UC	C	UC	C	UC	C	UC	C	UC	C	UC	C
1	0.68	0.25	0.75	0.32	0.88	0.25	0.63	0.28	0.89	0.21	0.51	0.37	0.86	0.32
2	0.62	0.22	0.82	0.23	0.78	0.23	0.83	0.24	0.86	0.22	0.59	0.36	0.86	0.29
3	0.55	0.22	0.65	0.21	0.65	0.22	0.82	0.26	0.87	0.24	0.42	0.37	0.71	0.30
4	0.56	0.22	0.60	0.21	0.52	0.24	0.79	0.27	0.77	0.24	0.47	0.40	0.55	0.29
5	0.71	0.24	0.53	0.20	0.47	0.25	0.68	0.26	0.77	0.24	0.63	0.39	0.53	0.26
6	0.84	0.23	0.74	0.24	0.81	0.22	0.85	0.31	0.87	0.26	0.89	0.39	0.83	0.26
7	0.72	0.24	0.67	0.29	0.84	0.24	0.83	0.32	0.81	0.28	0.78	0.34	0.86	0.27
8	0.56	0.21	0.85	0.29	0.63	0.25	0.72	0.28	0.66	0.26	0.68	0.29	0.72	0.23
9	0.58	0.17	0.85	0.31	0.63	0.27	0.58	0.25	0.61	0.26	0.52	0.22	0.56	0.20
10	0.50	0.11	0.63	0.21	0.37	0.20	0.41	0.23	0.41	0.21	0.42	0.15	0.41	0.14
Total	0.72	0.21	0.75	0.26	0.77	0.24	0.71	0.25	0.81	0.26	0.72	0.33	0.75	0.25

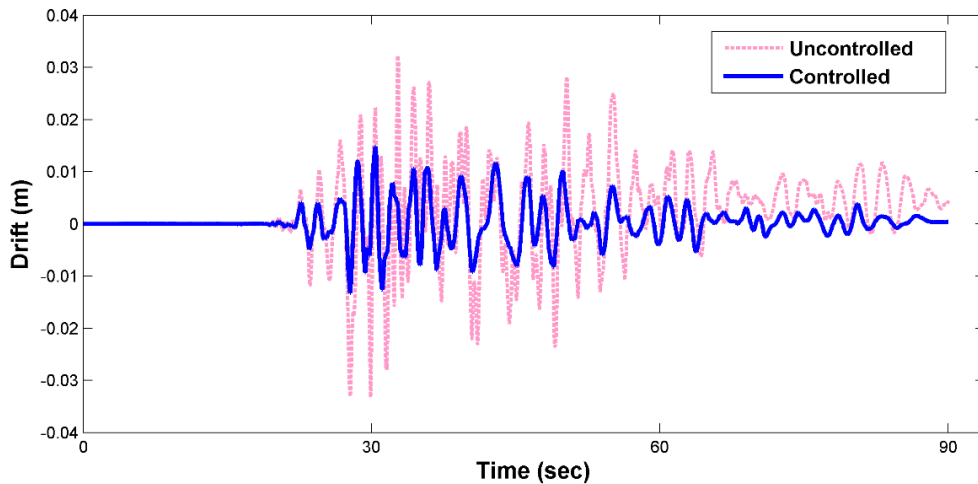


**Fig. 5 shows, for instance, the drift time-history of the first story of the 10-story building under Chi-Chi earthquake**

Meanwhile, in the calculations of Sec. 6, the control procedure was set to keep the story damages below 0.4. Then the results may be biased toward a *DI* of 0.4 and the estimation error of Eq. (16) might increase for larger *DI*s. However, it is not an important issue because an active control is implemented to keep the seismic damage in the repairable

range ( $DI \leq 0.4$ ) during a major earthquake event. It also has to be mentioned that Eq. (16) is valid only for the class of buildings studied, i.e., concrete moment frames up to ten stories with minor to medium (repairable) damage when they are actively controlled under large earthquakes.

Discrepancy of response data of Sec. 6 with regard to Eq. (16) is small. For example, the case of the 3-story building is presented here. Table 9 shows the exact (Eq. (2)) and estimated (Eq. (16)) damage indices in each story under each earthquake for the 3-story building. Wherever the estimated value of damage index is less than the exact value, the relative difference is shown as a negative number. It is seen that in all stories the average and maximum relative differences between the above *DI*s are both less than 10% showing the very good performance of Eq. (16) in estimation of *DI* or *u*, based on purpose, for the studied buildings.

At the first floor of the 6 and 10-story structures, the damage index estimated by Eq. (16) differs from the exact value by more than 10%. Numerical tests have shown that adding 0.05 to the value of the parameter *B* in the mentioned equation, i.e. modifying it to a new value of 0.0755 only in the mentioned locations, takes care of the problem.

### 8. APPLICATION OF THE DEVELOPED EQUATION

Equation (16) can be more confidently evaluated if use is

made of earthquake records different than the ones used in developing the same equation. Moreover, Eq. (16) is meant to be used for estimation of maximum drift of each story, based on the desired distribution of damage index. The estimated story drift is then utilized in the control algorithm. Therefore, in this section in order to show applicability of Eq. (16), the following three distributions of damage index are investigated:

- 1) Case I: A uniform distribution with  $DI=0.4$ ;
- 2) Case II: A uniform distribution with  $DI=0.2$ ;
- 3) Case III: A step distribution with  $DI=0.4$  in the lower half and  $DI=0.2$  in the upper half of building.

Four new earthquakes (different from Sec. 6) are utilized and 2 and 10-story buildings are analyzed. Therefore, applicability of Eq. (16) is assessed in 24 cases.

Criteria for selection of the new earthquakes are similar to Sec. 5.2. The selected records are scaled by trial and error such that the damage indices of the uncontrolled structures are in the range of 0.5-0.8 under the above earthquakes. Characteristics of the new earthquakes are mentioned in Table 10.

The 24 *DI*-structure-earthquake cases described above are analyzed. In each case, first Eq. (16) is used to estimate the maximum story drift based on the prescribed damage index in each story. Then values of the maximum story drifts are used in the control algorithm, explained in Sec. 3, to control the structures. The Park-Ang damage index is then calculated in each story under each earthquake using Eq. (2) and compared with the prescribed *DI*. This comparison determines the applicability of Eq. (16) in the active control algorithm utilized.

Tables 11-18 illustrate the results of analysis of this section. In each table, all three cases of the prescribed damage

**Table 9. Estimated and exact values of the damage index for the 3-story building**

Story number	Variable	Parkfield	Northridge	Loma Prieta	Kobe	Elcentro	Coalinga	Chi Chi	Average
1	Max drift (m)	0.0125	0.0168	0.0174	0.0114	0.0144	0.0158	0.0145	0.0146
	<i>DI</i> (Eq.16)	0.286	0.376	0.389	0.264	0.326	0.355	0.328	0.332
	<i>DI</i> (Eq. 2)	0.278	0.376	0.388	0.247	0.324	0.351	0.326	0.327
	Relative diff.(%)	3	0	0.3	6	1	2	1	2
2	Max drift (m)	0.0142	0.0163	0.0169	0.0164	0.0151	0.0166	0.0134	0.0155
	<i>DI</i> (Eq.16)	0.305	0.347	0.359	0.349	0.323	0.353	0.289	0.332
	<i>DI</i> (Eq. 2)	0.308	0.358	0.362	0.358	0.329	0.365	0.292	0.338
	Relative diff.(%)	-1	-3	-1	-3	-2	-3	-1	-2
3	Max drift (m)	0.0094	0.0108	0.0159	0.0074	0.0072	0.0076	0.0055	0.0090
	<i>DI</i> (Eq.16)	0.198	0.224	0.307	0.161	0.156	0.164	0.124	0.190
	<i>DI</i> (Eq. 2)	0.196	0.236	0.329	0.177	0.152	0.158	0.113	0.194
	Relative diff.(%)	1	-5	-7	-9	3	4	9	-2

**Table 10. Characteristics of the earthquakes selected for evaluation of Eq. (16)**

Earthquake name	Year	Station	PGA (g)
Morgan Hill	1984	CDMG 57382 Gilroy Array #4	0.224
San Fernando	1971	CDMG 24303 LA- Hollywood Stor FF	0.21
Northern	1954	Ferndale City Hall	0.203
Big Bear	1992	Desert Hot Springs	0.225



**Table 11. Comparison of the prescribed and calculated damage indices after nonlinear dynamic analysis; 2-story building, Morgan Hill earthquake**

Story	Prescribed <i>DI</i>	Max. drift (m) (Eq. 16)	Park-Ang <i>DI</i> (Eq. 2)	Relative difference of <i>DIs</i> (%)
1	Case I	0.0083	0.188	-6
	Case II	0.0179	0.404	1
	Case III	0.0179	0.410	2
2	Case I	0.0088	0.200	0
	Case II	0.0189	0.402	1
	Case III	0.0088	0.193	-3

**Table 12. Comparison of the prescribed and calculated damage indices after nonlinear dynamic analysis; 2-story building, San Fernando earthquake**

Story	Prescribed <i>DI</i>	Max. drift (m) (Eq. 16)	Park-Ang <i>DI</i> (Eq. 2)	Relative difference of <i>DIs</i> (%)
1	Case I	0.0083	0.191	-4
	Case II	0.0179	0.402	1
	Case III	0.0179	0.411	2
2	Case I	0.0088	0.188	-6
	Case II	0.0189	0.409	2
	Case III	0.0088	0.187	-6

**Table 13. Comparison of the prescribed and calculated damage indices after nonlinear dynamic analysis; 2-story building, Northern earthquake**

Story	Prescribed <i>DI</i>	Max. drift (m) (Eq. 16)	Park-Ang <i>DI</i> (Eq. 2)	Relative difference of <i>DIs</i> (%)
1	Case I	0.0088	0.195	-2
	Case II	0.0179	0.406	2
	Case III	0.018	0.409	2
2	Case I	0.0086	0.1901	-5
	Case II	0.0105	0.226	-43
	Case III	0.0086	0.182	-9

**Table 14. Comparison of the prescribed and calculated damage indices after nonlinear dynamic analysis; 2-story building, Big Bear earthquake**

Story	Prescribed <i>DI</i>	Max. drift (m) (Eq. 16)	Park-Ang <i>DI</i> (Eq. 2)	Relative difference of <i>DIs</i> (%)
1	Case I	0.0087	0.193	-4
	Case II	0.018	0.405	1
	Case III	0.018	0.405	1
2	Case I	0.0078	0.170	-14
	Case II	0.0098	0.211	-47
	Case III	0.0088	0.191	-5

distribution are mentioned.

Although totally new earthquakes are adopted, Tables 11-18 show that the active control procedure developed in this study along with Eq. (16), has been successful to prevail a desired distribution of damage index along height of the buildings. As seen, there are cases in which the difference between the target and actually gained damage index is more than 10%. However, in all of those cases, the actual damage index is smaller than the target and is thus in the safe side. Therefore, this procedure can be used at least as an estimative

procedure, in active control of reinforced concrete structures up to 10 stories.

As a final note, it should be noticed that according to the text after Table 3 and before Table 10, the structures designed using the current building codes showed more or less a repairable damage state under the selected strong earthquakes. Then the records had to be scaled up by a factor being in the range of 1.5-1.8 in order to increase the damage extent to an irreparable state. Such a factor corresponds approximately to the maximum credible earthquake (MCE). This is itself a very

**Table 15. Comparison of the prescribed and calculated damage indices after nonlinear dynamic analysis; 10-story building, Morgan Hill earthquake**

Story	Prescribed DI	Max. drift (m) (Eq. 16)	Park-Ang DI (Eq. 2)	Relative difference of DIs (%)
1	Case I	0.0059	0.205	2
	Case II	0.0155	0.370	-7
	Case III	0.0155	0.401	0
2	Case I	0.0088	0.211	5
	Case II	0.0189	0.367	-9
	Case III	0.0189	0.409	2
3	Case I	0.0094	0.204	2
	Case II	0.0200	0.369	-8
	Case III	0.0200	0.382	-5
4	Case I	0.0101	0.196	-2
	Case II	0.0213	0.376	-6
	Case III	0.0213	0.395	-2
5	Case I	0.0109	0.181	-9
	Case II	0.0227	0.364	-9
	Case III	0.0227	0.372	-7
6	Case I	0.0117	0.181	-9
	Case II	0.0242	0.412	3
	Case III	0.0117	0.194	-3
7	Case I	0.0126	0.184	-9
	Case II	0.0260	0.416	4
	Case III	0.0126	0.202	1
8	Case I	0.0137	0.208	4
	Case II	0.0280	0.392	-2
	Case III	0.0137	0.206	3
9	Case I	0.0150	0.216	8
	Case II	0.0304	0.364	-9
	Case III	0.0150	0.213	6
10	Case I	0.0164	0.167	-17
	Case II	0.0331	0.242	-40
	Case III	0.0164	0.162	-19

**Table 17. Comparison of the prescribed and calculated damage indices after nonlinear dynamic analysis; 10-story building, Northern earthquake**

Story	Prescribed DI	Max. drift (m) (Eq. 16)	Park-Ang DI (Eq. 2)	Relative difference of DIs (%)
1	Case I	0.0058	0.184	-8
	Case II	0.0137	0.372	-7
	Case III	0.015	0.391	-2
2	Case I	0.0084	0.195	-3
	Case II	0.0192	0.409	2
	Case III	0.0192	0.405	1
3	Case I	0.0091	0.199	-1
	Case II	0.203	0.403	1
	Case III	0.0199	0.403	1
4	Case I	0.0106	0.212	6
	Case II	0.203	0.381	-5
	Case III	0.0206	0.40	0
5	Case I	0.0118	0.214	7
	Case II	0.207	0.377	-6
	Case III	0.0204	0.363	-9
6	Case I	0.0124	0.213	7
	Case II	0.0245	0.41	3
	Case III	0.012	0.206	3
7	Case I	0.0127	0.202	1
	Case II	0.0263	0.409	2
	Case III	0.0118	0.193	-3
8	Case I	0.0131	0.193	-4
	Case II	0.0273	0.395	-1
	Case III	0.0128	0.181	-10
9	Case I	0.0134	0.187	-7
	Case II	0.0229	0.302	-25
	Case III	0.0136	0.172	-14
10	Case I	0.0142	0.179	-11
	Case II	0.0167	0.1935	-52
	Case III	0.0129	0.146	-27

**Table 16. Comparison of the prescribed and calculated damage indices after nonlinear dynamic analysis; 10-story building, San Fernando earthquake**

Story	Prescribed DI	Max. drift (m) (Eq. 16)	Park-Ang DI (Eq. 2)	Relative difference of DIs (%)
1	Case I	0.0059	0.205	2
	Case II	0.0155	0.363	-9
	Case III	0.0155	0.401	1
2	Case I	0.0088	0.211	5
	Case II	0.0189	0.382	-4
	Case III	0.0189	0.409	2
3	Case I	0.0094	0.204	2
	Case II	0.0200	0.395	-1
	Case III	0.0200	0.382	-5
4	Case I	0.0101	0.196	-2
	Case II	0.0213	0.386	-4
	Case III	0.0213	0.395	-2
5	Case I	0.0109	0.181	-9
	Case II	0.0227	0.384	-4
	Case III	0.0227	0.372	-7
6	Case I	0.0117	0.177	-11
	Case II	0.0242	0.410	3
	Case III	0.0117	0.194	-3
7	Case I	0.0126	0.179	-11
	Case II	0.0260	0.396	-1
	Case III	0.0126	0.202	1
8	Case I	0.0137	0.208	4
	Case II	0.0280	0.371	-7
	Case III	0.0137	0.206	3
9	Case I	0.0150	0.216	8
	Case II	0.0304	0.301	-24
	Case III	0.0150	0.213	6
10	Case I	0.0164	0.167	-17
	Case II	0.0331	0.178	-55
	Case III	0.0164	0.163	-19

**Table 18. Comparison of the prescribed and calculated damage indices after nonlinear dynamic analysis; 10-story building, Big Bear earthquake**

Story	Prescribed DI	Max. drift (m) (Eq. 16)	Park-Ang DI (Eq. 2)	Relative difference of DIs (%)
1	Case I	0.0055	0.172	-14
	Case II	0.0152	0.403	1
	Case III	0.0104	0.308	-23
2	Case I	0.0086	0.186	-7
	Case II	0.0189	0.389	-3
	Case III	0.0147	0.313	-22
3	Case I	0.0094	0.188	-6
	Case II	0.019	0.384	-4
	Case III	0.0158	0.33	-18
4	Case I	0.0104	0.197	-2
	Case II	0.0213	0.398	-1
	Case III	0.0156	0.295	-26
5	Case I	0.0111	0.203	2
	Case II	0.0203	0.368	-8
	Case III	0.0117	0.218	-45
6	Case I	0.0110	0.182	-9
	Case II	0.0232	0.395	-1
	Case III	0.0121	0.201	1
7	Case I	0.0112	0.177	-12
	Case II	0.0238	0.377	-5.75
	Case III	0.013	0.198	-1
8	Case I	0.0115	0.165	-18
	Case II	0.0242	0.352	-12
	Case III	0.0133	0.197	-2
9	Case I	0.0116	0.159	-21
	Case II	0.0237	0.305	-24
	Case III	0.0155	0.208	4
10	Case I	0.0123	0.153	-24
	Case II	0.0167	0.21	-48
	Case III	0.0133	0.158	-21

clear verification since the mentioned damage behavior is completely in line with the intent of the current seismic codes and shows how good the design and nonlinear behavior of the studied buildings resemble the expectations. Moreover, as seen in Tables 4-8, the dispersion of the damage index values is limited and all the values fluctuate around a closely spaced average. Tables 11-18 confirm that the observations of Tables 4-8 have not been accidental, as almost the same findings are gained with a completely different set of earthquakes. All of the above facts together establish the rationality and correctness of the research calculations.

## 9. CONCLUSIONS

In this paper an active control procedure based on the LQR algorithm was used to actively control buildings having up to 10 stories. The target was limiting the story damage index to a prescribed value. Since the above algorithm needs the maximum acceptable story drifts as its prerequisite, the story drifts associated with a prescribed damage index were calculated by trial and error. In this step, seven consistent earthquake records were used for nonlinear dynamic analysis of concrete structures being 1, 2, 3, 6 and 10 stories tall. The control procedure was shown to be successful in keeping the story damage indices below the prescribed value. Then through a curve fitting process, a regression equation was developed using the data of the above analysis, to maintain a relation between the maximum story drifts and the damage index in each story.

The discrepancy of the data with regard to the developed equation was shown to be small as the maximum relative difference between the estimated and exact damage indices was less than 10%. The developed *DI* equation was also successful when it was used within the control process to determine the acceptable maximum story drifts for a prescribed distribution of damage index along building height. Four earthquake records, different from the suit of ground motions used for developing the *DI* equation, were used for the above purpose. It was shown that by using the story drifts estimated by the developed equation, the desired distribution of story damage indices can be established with a very good accuracy. Wherever the difference between the target and actual drifts grew, the actual one was always on the safe side, i.e., smaller than the target drift.

## REFERENCES

ASCE/SEI 7-10 (2010) Minimum design loads for buildings and other structures.  
Attard, TL, Wharton, CR (2012) Optimal control parameterization for displacement and acceleration demands and local post-yield constitutive

responses. *Engineering Structures* 36(1): 123-133.  
Baghban, A, Karamodin, A, Haji-Kazemi, H, (2015), Nonlinear control of structure using neuro-predictive algorithm. *Smart Structures and Systems* 16 (6): 1133-1145.  
Chu, SY, Soong, TT, Reinhorn, AM (2005), *Active, Hybrid, and Semi-active Structural Control: A Design and Implementation Handbook*, Wiley, New York, NY, USA.  
Datta, TK (2003) A state-of-the-art review on active structure control. *Journal of Earthquake Technology* 40(1): 1-17.  
Housner, GW, Bergman, LA, Caughey, TK, Chassiakos, AG, Claus, RO, Masri, SF, Skelton, RE, Soong, TT, Spencer, BF, Yao, JTP (1997) *Structural control: past, present, and future*. *Journal of Engineering Mechanics* 123(9): 897-971.  
Joghataie, A, Mohebbi, M (2012) Optimal control of nonlinear frames by Newmark and distributed genetic algorithm. *The Structural Design of Tall and Special Buildings* 21(2): 77-95.  
Karami Mohammadi, R, Haghhighipour, F (2017), Implementation of Uniform Deformation Theory in semi-active control of structures using fuzzy controller. *Smart Structures and Systems* 19(4): 351-360.  
KhanSefid, A, Ahmadizadeh, M (2016), An investigation of the effects of structural nonlinearity on the seismic performance degradation of active and passive control systems used for supplemental energy dissipation. *Journal of Vibration and Control* 22 (16), 3544-3554.  
KhanSefid, A, Bakhshi, A (2018), Advanced two-step integrated optimization of actively controlled nonlinear structure under mainshock-aftershock sequences. *Journal of Vibration and Control*, Vol. 25, Issue 4, 1-15.  
Kunnath, SK, Reinhorn, AM, Lobo RF (1992) IDARC version 3: A program for the inelastic damage analysis of RC structures. Technical report NCEER-92-0022. Buffalo (NY): National Center for Earthquake Engineering Research, State University of New York.  
Miyamoto, K, Sato, D, She, J, (2018), A new performance index of LQR for combination of passive base isolation and active structural control. *Engineering Structures* 157(15): 280-299.  
Miyamoto, K, She, J, D, Sato, Yasuo, N, (2018), Automatic determination of LQR weighting matrices for active structural control. *Engineering Structures* 174(1): 308-321.  
OpenSees (2014). *Open System for Earthquake Engineering Simulation, Version 2.4.2*. Pacific Earthquake Engineering Research Center.  
Pang, M, Wong, K (2006) Predictive instantaneous optimal control of inelastic structures based on ground velocity. *The Structural Design of Tall and Special Buildings* 15(3): 307-324.  
Park, YJ, Ang AHS (1985), Seismic damage analysis of reinforced Concrete buildings. *Journal of Structural Engineering* 111(4): 740-757.  
PEER (2014). Pacific Earthquake Engineering Research Center, <http://peer.berkeley.edu/index.html>.  
Shooshtari, M, Saaticioglu, M (2003), *Active Structural Control of Concrete Structures for Earthquake Effects*, *Proceedings of the 13th World Conference on Earthquake Engineering*, Vancouver, Canada, August.  
Soong, T. T. (1990) *Active Structural Control: Theory and Practice*, Longman Scientific and Technical, New York, NY, USA.  
Varaste, A, Behnamfar, F, Salimi, M (2012), Assessment of the conventional control algorithms and proposing a modified displacement feedback control for performance-based design of structures. *Computational Methods in Civil Engineering* 3(1): 35-50.  
Williams, MS, Sexsmith, RG (1995), Seismic damage indices concrete structures: a state-of-the-art review. *Earthquake Spectra* 11(2): 319-349.  
Yang, J, Wu, J, Li, Z (1996), Control of seismic-excited buildings using active variable stiffness systems. *Engineering Structures* 18(8): 589-596.

### HOW TO CITE THIS ARTICLE

MS. Kazemi, F. Behnamfar, *Active control of structures based on an arbitrary damage index distribution*, *AUT J. Civil Eng.*, 4(3) (2020) 385-396.

DOI: [10.22060/ajce.2019.16680.5598](https://doi.org/10.22060/ajce.2019.16680.5598)



